Graphene-Based Cementitious Composites: Toward Next-Generation Construction Technologies

Malgorzata Krystek, Artur Ciesielski, Paolo Samorì

WILEY-VCH

Graphene-based cementitious composites: Towards next-generation construction technologies

Małgorzata Krystek, Artur Ciesielski, Paolo Samorì**

Dr. M. Krystek, Dr. A. Ciesielski, Prof. P. Samorì
Université de Strasbourg, CNRS, ISIS, 8 alleé Gaspard Monge, 67000 Strasbourg, France
E-mail: ciesielski@unistra.fr; samori@unistra.fr

Dr. M. Krystek
Department of Structural Engineering, Faculty of Civil Engineering, Silesian University of Technology, Akademicka 5, 44-100 Gliwice, Poland

Keywords: cement, electrical properties, graphene, hydration, mechanical properties, microstructure

Abstract

The search for technological solutions to the ever-increasing demand towards the use of ultra-high-quality concrete with simultaneous construction boom represents one of the greatest challenges concrete researchers are facing nowadays. In view of their unique properties, graphene and related materials, when utilized to form graphene-based cementitious composites, appear as most powerful components to give a boost to today's concrete technology. In this Review, we showcase the most enlightening recent advancements in the development of fabrication protocols for obtaining the homogenous dispersion of graphene and derivatives thereof within cement matrix. We also discuss the hydration process and basic properties of graphene-based cementitious materials. The integration of graphene-family materials to concrete technology allows to impart new functions to cement composites towards the construction of smart and multifunctional buildings. Therefore, a specific focus will be given to the electrical and piezoresistive behavior of graphene-cement composites, and ultimately their great potential for Structural Health Monitoring applications. The approaches proposed in this review can be also extended to other 2D materials offering a broadest arsenal of physical properties, which can therefore be integrated on-demand in future smart structures and constructions.

1. Introduction

Concrete, with its global production of 10 billion cubic meters per year,[1] is the world's most consumed material. Because of its unique properties and simplicity of use, concrete is the most widely employed man-made material in structural engineering and the most critical construction component in today's rapidly urbanizing world.[2,3] Nowadays colossal research endeavors are continuously devoted to enhancing the performance of cementitious composites. This is because while a construction boom incessantly increases concrete consumption, concrete structures still suffer from several significant drawbacks strictly related to the intrinsically defective nature of cement composites.[3] More specifically, concrete exhibits low tensile strength, i.e. from 2.2 MPa to 5.0 MPa for concrete classes C20/25 – C90/105 (the average value),[4] which accounts for 5-8% of its compressive strength (the average values in the range of 28-98 MPa), leading to the inherent quasi-brittle behavior with high vulnerability to cracking. As a result, the harsh atmospheric conditions as well as the presence of aggressive and harmful ions (in particular carbonate, chloride and sulphate ions) easily affect the microstructure of cement composites, thus initiating the corrosion and degradation of concrete structures.[5] This entails the highly increased maintenance costs of concrete buildings, since expensive actions need to be taken in order to avoid the construction failure and preserve the safety of building's user. Alongside, considering the largest-scale use of concrete, the environmental hazards, such as CO_2 emission, non-renewable resource scarcity and energy consumption, are gaining a great deal of attention all over the world.[1,2,6] All these aspects force engineers and scientists to continually seek out for novel, unconventional compositions of cement composites, whose performances could boost the evolution of concrete technology and contribute in reducing the consumption of concrete components.

Fundamentally, concrete is a composite material composed of the fine and coarse aggregate grains embedded into a solid matrix formed by chemical, physical or

physicochemical reactions occurring between the binder and water.[7,8] Indeed, the binder is the most critical concrete component playing the paramount role in determining the final properties and applications of concrete. Although different types of binders may be applied in concrete, including organic binders, such as asphalt and polymers, or nonhydraulic inorganic ones, namely lime and gypsum, it is cement, i.e., the hydraulic inorganic material, that is the most commonly adopted binder to manufacture ordinary concrete. Depending on the required properties, the construction conditions or the designed application, five main types of products build the family of common cements: Portland cement (CEM I), Portland cement with supplementary materials, in particular blast furnace slag, fly ash, pozzolana, limestone and silica fume (CEM II), blast furnace cement (CEM III), pozzolanic cement (CEM IV) and composite cement (CEM V). [7,8] Although the application of supplementary cementitious materials offers the possibility to meticulously tailor the selected properties of fresh concrete mix or hardened composites, the ordinary Portland cement still remains the most widely employed concrete binder.

To date, concrete building blocks are typically reinforced with steel rebars or various types of fibers, including carbon, steel, glass and polypropylene.[3,9] In such structures, the bending moment and shear resistance can be meticulously programmed. Furthermore, such reinforcement enable to achieve a greater control over the initiation and propagation of cracks. Nevertheless, the use of microfibers has some drawbacks related to the reduced workability of fresh concrete mix and entrained air voids within cement matrix.[10] Moreover, such types of reinforcement do not affect the cement hydration products, thereby the brittleness and cracking still occur at the nano-scale.[3] Such short comings, along with the ever-increasing demand towards lighter and more slender concrete structures have triggered immense research endeavors on the use of nanostructured materials in concrete structures. Indeed, the effect of nanoadditives on microstructure and properties of cementitious composites has been explored by numerous researchers during the last two decades.[11,12] The

incorporation of nanomaterials into cement matrix offers a wide range of potential improvements: from the major changes in already existing properties of cement composites up to the development of radically new and unique functionalities. Although plethora of different nanomaterials, such as nanosilica, nanotitania, nanoalumina or carbon nanotubes, has been applied in cement composites so far,[12] it is graphene, an exciting 2D carbon material presenting a largest portfolio of outstanding characteristics,[13–15] that seems to open up new remarkable avenues for the next generation of concrete technologies.

Graphene is an attractive 2D nanomaterial which has revolutionized the field of nanoscience and nanotechnology due its unprecedented properties, in particular its remarkable electrical properties, mechanical strength and flexibility.[13–15] During the last few years, major step forwards have been made on the production of graphene and related materials by improving the quantity and quality, also *via* the tailoring of their properties. Nevertheless, the production of novel cementitious composites incorporating nanoadditives still involves the perplexing problem of disentanglement and homogenous dispersion of nanoparticles within cement matrix. In particular, carbon two-dimensional materials tend to form agglomerates and yields to flocculation in aqueous environment due to strong van der Waals forces and/or their hydrophobic nature.[16]

Initially, graphene oxide (GO) was identified as novel 2D material for concrete technology owing to its low-cost production, easy processability and high dispersibility in water.[17] As a result, the development of GO-cement composites has been the subject of previous review articles,[10,18–23] whereas only a few works[18–21] have considered the use in cementitious composites of other graphene related materials such as graphene nanoplatelets (GNPs), reduced graphene oxide (rGO), multi-layer graphene (MLG) or few-layer graphene (FLG) which possess different chemical, structural and physical properties. In this framework, a central point of this Review is a critical comparison of the potential benefits and drawbacks of the application of different graphene derivatives in cement-based materials. Towards this

end, we will highlight the problems associated to obtaining uniform dispersion of graphene and its derivatives within cement matrix through the optimization of complex processes for the fabrication of graphene/cement composites (Section 2). The mechanical properties of as produced composites as well as their durability, microstructure and cement hydration are further discussed in Section 3.

Nanomaterials have high production costs when compared to plain concrete mix and they require complex protocols to ensure their proper dispersion within cement matrix, thus limiting to a large extent their application in a real scale concrete structure. The real added value in concrete technology is represented by unique and exceptional smart functionalities that are imparted by the nanomaterials, i.e. self-sensing, self-cleaning, antimicrobial, anticorrosion or air purifying abilities,[12] rather than by just through the improvement of the existing properties of cement composites. In particular, the concept of internal conductive network originating from conductive nanomaterials enabling real time monitoring of strain, stress, cracks or damage makes self-sensing concrete a viable strategy for Structural Health Monitoring (SHM) of concrete structures. Nevertheless, while the effect of graphene and derivatives thereof on the microstructure, mechanical properties and durability of cementitious composites has been the subject of a few review articles so far,[10,18–23] the concept of potential self-sensing capability of graphene-based cementitious composites, which appears as the key to revolutionize concrete structures, have been disregarded. To fill this gap, we also extend the scope of this Review to the discussion on the electrical and piezoresistive properties of graphene/cement composites and their potential applications in SHM of concrete structures (Section 4). We will discuss thoroughly the importance of imparting additional functions to the buildings via integrating self-sensing mechanisms occurring in graphene-cement composites. It is our intention to provide the scientific community with a comprehensive guideline to design cement composites for smart and multifunctional buildings

structures and therefore to offer a real practical application to many nanostructured materials already available.

2. Fabrication protocols for graphene-based cementitious composites

The incorporation of any nanomaterials into cement composites requires their homogeneous dispersion within cement matrix, since if nonuniformly dispersed they could be detrimental to the overall microstructure, mechanical properties and durability of cement-based composites. Such a task is even more challenging in case of two-dimensional materials (2DMs) due to the perplexing dispersion problems inherited from strong van der Waals forces and/or hydrophobic nature of 2DMs.[16] Therefore, the ease of obtaining the high-quality GO dispersion in aqueous environment (**Figure 1**a) arising from the oxygen functional groups exposed on the basal plane and on the edges of the nanosheets[16,17] made GO the most studied graphene derivative in concrete nanotechnology. Indeed, since the pioneering study reported in 2013,[24] the early stages of the research on GO-cement composites have relied exclusively on ultrasonication of GO dispersion in water, prior to mixing with cement,[25–33] yet, this technique manifests one major drawback concerning the deterioration of rheological parameters of fresh cement paste and the notable reduction of its workability. The reduction of fluidity by means of the mini-slump test as high as 32.1%[34] and 41.7%[35] was achieved for GO loadings of 0.03 wt.% and 0.05 wt.% (solid dosage and by weight of cement), respectively. Wang et al.[34] have reported on the rheological properties of cement paste incorporating 0.03 wt.% of GO: the yield stress and apparent viscosity were drastically increased by 82.1% and 33.6%, respectively. In a similar vein, Lu et al.[31] have observed the significant decrease of initial and final setting time of GO-cement paste. By and large, the authors attributed this phenomenon to the large specific surface area of GO sheets absorbing more water to wet their surface rather than the surface of cement particles.[31,34,36]

Nonetheless, as revealed by later studies,[31,37–39] the stable, homogenous aqueous dispersion of GO is no longer stable in cement environment. In fact, the incorporation of GO dispersion into cement mix entails the immediate formation of flocculation and agglomerations entrapping free water molecules (Figure 1b), thus deteriorating the fluidity and rheological properties of cement composites. This phenomenon is driven by the formation of metal complexes, i.e. chemical cross-linking between oxygen functional groups of GO sheets and calcium ions originating from cement.[31,37,38] Recently, it has been also shown that the scenario becomes even more complicated due to highly alkaline cement environment, which leads to the deprotonation of GO carboxyl groups increasing the amount of adsorbed Ca^{2+} ions.[40]

Therefore, in order to overcome this limitation, various fabrication protocols for GO-cement composites have been developed and pursued during the last few years to foster the homogenous dispersion of graphene oxide within cement matrix. In particular, the overwhelming majority of cementitious composites incorporating GO derive from surfactant-assisted dispersion techniques.[37,39–43] This approach involves the surface modification of GO by its sonication in the presence of surfactants, preferably polycarboxylate superplasticizers (PCs), i.e. comb-like copolymers with grafted polyoxyalkylene groups chains, prior to adding cement (Figure 1c).[41] The main advantages of this strategy lie with the superior aptitude of PCs in providing the steric repulsion between GO nanosheets, as depicted in Figure 1d, along with the steric hindrance effect separating GO sheets from charged ions.[40–42] Nevertheless, such an approach is accompanied by some drawbacks related to the appropriate choice of surfactant type and dispersion protocol. On the one hand, it was proved that the efficiency of the steric stabilization effect highly depends on the molecular structure of the polymer, i.e. the length of its side chains and its charge density.[37,44] On the other hand, the quality of GO dispersion strongly relies on the sonication frequency (viz. energy) and the time at which PC is introduced into the dispersion.[44] Moreover, the studies of Lu et al.[42] have indicated the

crucial importance of the PC amount incorporated into cement matrix. While the PC dosage is higher than the certain critical concentration, the formation of micelles reducing the apparent surfactant concentration occurs, thereby negatively affecting GO dispersion (Figure 1e).

Another intriguing method towards the fabrication of GO-cement composites relies on the use of silica fume in order to separate GO sheets from charged ions. Here, three major techniques are applied: (1) mechanical mixing of silica fume with GO water dispersion, prior to cement addition,[38] (2) the incorporation of GO encapsulated silica fume particles,[45] and (3) the deposition of nanosilica particles on GO nanosheets *via* a sol-gel method by *in situ* hydrolysis and condensation of tetraethylorthosilicate (**Figure 2**a).[46–48] Analogously, Wang et al.[34] have reported that also the addition of fly ash prevents the flocculation of GO, thus increasing the fluidity of GO-cement mix. Moreover, the chemical functionalization of GO with polyether amines (Figure 2b),[49] coating of cement particles with GO in isopropanol suspension[50] and using the edge-oxidized GO produced by ball-milling treatment[51] (Figure 2c) represent additional valuable, yet complex methods developed recently for the fabrication of GO-cement composites.

Although the oxygen functional groups of GO nanosheets contribute to its high dispersibility in water as well as provide reactive sites for a variety of reactions allowing to develop a broad arsenal of unique GO-based composites, these functional groups entail as well the disruption of the electronic structure with the formation of irreversible in plane defects and disorders, thus GO becomes electrically insulting and features with significantly lower strength and elastic modulus, if compared to pristine graphene.[16] From this perspective, other graphene-family materials, such as reduced graphene oxide, graphene nanoplatelets, few-layer graphene and multi-layer graphene have been recently applied in cement composites to superiorly foster their mechanical and electrical properties. Noteworthy, the development of a fabrication protocol for cement composites incorporating rGO, GNPs, FLG or MLG allowing both the uniform dispersion of graphene nanosheets within cement

matrix and the appropriate workability is even more challenging, compared to GO, due to the intrinsic hydrophobicity of graphene flakes.[52] However, similarly to GO, the most commonly adopted strategy involves the use of ultrasonication and surfactants, e.g. naphthalene sulfonate,[53–55] melamine,[54,56,57] polycarboxylate,[36,54,58–61] sodium dodecyl sulfate,[59,62,63] sodium dodecyl benzene sulfonate,[59,62] hexadecyl trimethyl ammonium bromide,[62] methylcellulose[64] or N-dimethylacetamide[62] among others (**Figure 3**a). Noteworthy, some attempts of the fabrication of cement composites incorporating the aqueous dispersion of GNPs[65] and monolayer graphene[32] have been also reported. However, this strategy turned out not to be the most favorable one, since these composites emerged as materials with drastically deteriorated microstructure and properties. Intriguingly, the successful fabrication of the surfactant-free cementitious composites containing multi-layer graphene was proved by Silva et al.[66] as well as by Dela Vega and Vasquez.[67] The former incorporates graphene synthesized by the exfoliation of expanded graphite flakes in isopropanol, while the latter involves the use of MLGs obtained *via* liquid-phase exfoliation of O_2 plasma-functionalized graphite flakes, where O_2 functional groups attached to graphene nanosheets after plasma functionalization (Figure 3b) inhibit their agglomeration and thus ensure high stability of the dispersion. Recently, we have reported the generation of a novel cementitious mortar incorporating a few-layer graphene nanosheets obtained *via* electrochemical exfoliation of graphite, which is produced by dry-mixing of cement and graphene, prior to water addition, without the use of surfactants. Electrochemically exfoliated graphene proved not to aggregate in alkaline environment and thus does not affect the fluidity of fresh cement composites. The addition of 0.05 wt% of graphene to ordinary Portland cement resulted in a remarkable increase of the tensile strength up to 79% and further structural characterization shown that graphene accelerates cement hydration, thus resulting in high formation of C-S-H phase, as well as much more compact and regular microstructure of cement mortars.[68,69]

3. Microstructure-properties relationship in graphene-based cementitious composites

3.1. GO

A great effort in the field of graphene-based cement composites is incessantly devoted to the assessment of their mechanical properties, which are among the most crucial properties for structural applications of building materials. Nevertheless, even though the mechanical behavior of GO-cement composites has been extensively investigated to date, the effect of graphene oxide on the strength of cement composites has not yet been fully clarified. In general, it has been extensively proved that extremely low GO loadings, i.e. from 0.02 wt.% to 0.08 wt.%, might enhance significantly the strength of Portland cement composites. The maximum increase of the 28-day compressive, flexural and tensile strength up to 46.8%,[30] 83%[70] and 67.0%,[33] respectively, has been reported so far for composites incorporating aqueous GO dispersion (without the use of surfactants), while the corresponding values obtained for composites produced with the use of PCEs are 47.9%, 60.7% and 78.6%,[24] respectively. However, it should be pointed out that the values vary notably from study to study: although a few studies have shown the improvement of compressive strength in the range of 46-48%,[24,30,71] the average increase accounts mostly to 10-25%.[28,36,39,45,47] In fact, these findings cannot be directly compared due to the significant variations in composites composition and experimental procedures. In particular, the results of strength tests are strongly affected by GO morphology (lateral size and thickness of nanosheets), oxidation level of GO, GO dispersion method, type and amount of surfactant, if used, water-to-cement ratio, use of any additives, specimen size and type or loading rate. Recently, the seminal work published by Jing et al.,[72] on the visual spatial distribution of GO agglomerates and pore phases within cement matrix investigated *via* micro computed tomography (micro-CT), has provided evidence for the limited dispersion ability of PCs. The 3D visualization of the GO-cement specimens has revealed many irregular GO agglomerates with arbitrary flat shape

randomly dispersed within cement matrix (**Figure 4**a). This provides an additional explanation to the variable effect of GO nanosheets on the mechanical properties of cement composites within different studies.

In order to understand the origin of the improvement of mechanical properties as well as the underlaying strengthening mechanism of GO, a tremendous effort is devoted to the investigation of hydration process, microstructure and composition of GO-based cementitious composites. Initially, the rate of hydration heat development has been explored[30,36,73–75] by means of isothermal calorimetry, which provides direct insight into the early-age hydration kinetics of cementitious composites. The GO-cement pastes feature with higher dissolution rate,[30] hydration rate[30,36] as well as cumulative heat flow,[30,36,73] if compared to plain composites, being an indication of accelerated early-age cement hydration and rapid nucleation of hydration crystals, albeit this effect may be also temporarily retarded, if PC is used to disperse GO nanosheets.[74,75] According to Li et al.,[30] the hydration heat rate scales proportionally with the increase of GO loading, with higher magnitude of peaks in the hydration heat curve and the visible shift of the second peak suggesting the decreased hydration time (Figure 4b). Indeed, the calorimetric observations are confirmed by the mechanical tests: the highest increase of the strength of GO-cement composites is typically noted for early stages of cement hydration. Zhao et al.[41] have demonstrated GO-reinforced cement mortar exhibiting the compressive strength increased by 34.1%, 26.9% and 22.6% after 3, 7 and 28 days of hydration, respectively. In a similar vein, Yan et al.[44] have recently reported the increase of the compressive and flexural strength of cement mortar incorporating 0.02 wt.% of GO in the ranges of 14-16% for 3-day specimens, 5-7% for 7-day specimens and only 3-5% in case of samples cured for 28 days.

Apart from the early stages of cement hydration, the conflicting results of microstructural characterization and thus a variety of possible strengthening mechanisms of GO in cement composites have been reported in the literature. On the one hand, the improved

mechanical properties of GO-cement composites have been attributed to the enhanced hydration degree, since higher formation of $Ca(OH)_2$ and $3CaO{\cdot}2SiO_2{\cdot}3H_2O$ (C-S-H) phases has been clearly observed in composites incorporating GO,[39,41] while no changes in C-S-H structure have been detected. On the other hand, Vallurupalli et al.[75] have suggested that GO contributes also in the extension of the chain length of C-S-H phase, whereas Wang et al.[28] have reported the highly reduced amount of $Ca(OH)_2$ in GO-cement composites suggesting the formation of a new hydration product $Ca(HCOO)_2$ formed by chemical interaction between calcium hydroxide and -COOH groups of GO. In this view, the authors have introduced a 3D structure of GO nanosheets linked by COO-Ca-OOC, with cement hydration products growing inside the 3D GO network (**Figure 5**a). However, the reduced $Ca(OH)_2$ content has been also ascribed to the accelerated formation of carboaluminate hydrates ($3CaO{\cdot}Al_2O_3{\cdot}CaCO_3{\cdot}11H_2O$) fostered by high chemical reactivity of GO,[25] since the hydration of tricalcium aluminate ($3CaO{\cdot}Al_2O_3$) turned out to be more affected by GO incorporation than the hydration of tricalcium silicate ($3CaO{\cdot}SiO_2$).[31] Alongside, Lv et al.[24] have indicated that GO active functional groups act as nucleation sites reacting preferentially with $3CaO{\cdot}SiO_2$, $2CaO{\cdot}SiO_2$ (dicalcium silicate) and $3CaO{\cdot}Al_2O_3$, thereby fostering the growth of flower-like hydration crystals on GO nanosheets (Figure 5b, c).

Overall, the incorporation of GO into cement composites results mainly in regular and compact microstructure[25,31,36,76] with inhibited propagation of cracks[41,77] and highly reduced porosity of cement skeleton.[36,74,77,78] The increased surface area from 27.3 m^2/g to 64.9 m^2/g,[35] the shift of the critical pore size from 830.3 nm to 120.5 nm[74] as well as the increased volume of small and medium pores with the simultaneous reduction of large pores have been reported for GO-cement composites so far (Figure 4c). The visible densification of the microstructure provides a rational explanation for the improved mechanical performance of GO-cement composites as well as indicates that GO may be adopted to enhance the

durability of cementitious composites, which is strongly associated with their liquid and gas transport properties and porosity. Indeed, with the introduction of GO nanosheets, water absorption of cementitious composites may be highly reduced;[27,77] in this regard, Mohammed et al.[27] have reported the decrease of the secondary sorptivity coefficient from 0.46 μm/s$^{1/2}$ to 0.20 μm/s$^{1/2}$ with 0.03 wt.% loading of GO. As a consequence, the chloride ions penetration depth was remarkably lowered from 26 mm to 5 mm. The restricted mobility of chloride ions is attributed not only to the refined porosity of cement matrix, but also to the trapping phenomenon occurring within the layered structure of GO nanosheets. The reduced porosity of GO-cement composites contributes also in the suppressed movement of CO_2 molecules with consequent inhibition of the carbonation process.[79] In particular, the dissolution of $Ca(OH)_2$ and the decalcification of C-S-H phase are highly minimized at the early stages of carbonation.[80] Moreover, the reduced carbonation rate is also associated with the interlocking of calcium and carbonate ions by GO sheets.

As aforementioned, an additional approach to fabricate GO-based cementitious composites relies on the use of silica fume, which plays a double role by ensuring the sufficient dispersion of GO and fluidity of fresh cement mix as well as by initiating the pozzolanic reaction, that is a reaction between silica fume and $Ca(OH)_2$ resulting in the formation of secondary C-S-H phase.[45–48] Nevertheless, the combination of GO and silica fume leads only to the slight increase of mechanical properties of cement composites: the maximum increase of the 28-day compressive, flexural and tensile strength up to 33%,[46] 35%[48] and 31%,[47] respectively, has been reported so far.

Ultimately, it should be emphasized that several studies[56,68,72] show the negligible or even detrimental effect of GO addition on the microstructure and mechanical properties of cementitious materials, most probably due to the insufficient dispersion of GO within cement matrix leading to randomly distributed large-sized GO aggregates disrupting cement hydration. In particular, Wang et al.[56] have presented cement pastes with GO nanosheets

dispersed with the use of melamine dispersant, which showed no major changes in cement hydration and featured with high irregularity of the microstructure with numerous macropores.

3.2. rGO

GO is widely known as a non-conductive graphene derivative possessing significantly lower mechanical properties, if compared to pristine graphene. Intuitively, since the chemical reduction of GO with the use of hydrazine hydrate or sodium borohydride may partially restore its conductivity and strength,[16] rGO seems to be a promising alternative for high-performance cementitious composites. However, the present research involving rGO-cement composites remains highly limited, while the studies already published[36,50,81] have shown that, due to the reduced number of oxygen functional groups, the beneficial effect of rGO on the performance of cement composites is strongly inhibited. In fact, few extensive comparisons[36,50,81] have revealed that rGO fosters cement hydration and affects positively the microstructure and mechanical properties of cement composites, yet, the effect of GO was far more favorable. Qureshi and Panesar[81] have investigated the rate of hydration heat in cementitious composites incorporating GO and rGO during first 72 h of cement hydration. Indeed, the peaks of heat flow for GO-cement composite were notably increased and shifted to the left (**Figure 6**a), indicating the highly accelerated hydration, while rGO did not affect the heat release and even slightly delayed the hydration process (Figure 6b).

Nevertheless, the influence of rGO on the microstructure and properties of cementitious composites may be tuned by playing with the sonication time and thus the size of rGO flakes. Kiamahalleh et al.[82] have revealed that by increasing the sonication time from 1h to 4h a reduction of the size of rGO sheets from 245 nm to 170 nm is observed. As a result, the 28-day tensile and compressive strength was remarkably increased by 52% and 91%, respectively.

Interestingly, Prabavathy et al.[83] have observed the markedly enhanced durability-related properties of rGO-cement mortar. In particular, the 0.1 wt.% loading of rGO resulted in the highly restricted water absorption and carbonation depth as well as significantly improved performance of cement composites subjected to high temperatures. Moreover, rGO offers also a great control over the formation of thermal cracks of cement composites by improving the heat propagation and thus minimizing the heat differences between the edges and the surface of cement mortar specimens, as reported by Jing et al.[84]. Clearly, Figure 6c shows that reference cement paste exhibited many high thermal flux regions, the indication of the non-uniform heat distribution, while the effective propagation of heat in time was achieved in rGO-cement samples where the distribution of heat flux appeared as relatively homogenous.

3.3. GNPs

The potential application of graphene nanoplatelets in cement composites have been assessed over the past years due to their unprecedented electrical and mechanical properties as well as relatively low cost.[85] Nevertheless, from the perspective of their mechanical properties, GNPs turned out not to be the most suitable graphene derivative. Indeed, the effect of GNPs on compressive and flexural strength of cement composites is mostly negligible, with the maximum increase of 13.5%[59] and 27.8%,[62] respectively. Although some researchers[54,64,86] have indicated that GNPs accelerate cement hydration and result in the high formation of $Ca(OH)_2$ and C-S-H phase, the mechanical properties tests show that, most likely, GNPs, due to their large size (as shown in **Figure 7**a), do not affect markedly the hydration process, and rather act as nanofillers in porous microstructure of cement composites and as nanoreinforcement inhibiting cracks development.[53,56,59] Moreover, the size of GNPs does not allow to sufficiently transfer stress between aggregate particles in cement mortars and concrete, and therefore the reinforcing role is strongly inhibited.[53]

A seminal work on the flexural behavior of cement mortar incorporating GNPs was published by Tragazikis et al.[58] Noteworthy, the 0.2 wt.% loading of GNPs reduced significantly the flexural strength of cement mortar by 42%. The authors attributed this behavior to the shape of graphene nanoplatelets and their random orientation within cement matrix: the flakes oriented perpendicularly to the beam neutral plane not only lose their reinforcing ability, but also impair the microstructure of cement composite negatively affecting the stress transfer along the specimen. Interestingly, the three-point bending tests with simultaneous acoustic emission monitoring have shown a tremendously increased fracture energy (by 1700%, Figure 7b) as well as the superior change from the brittle behavior of cement composites to more ductile response, being a fingerprint of the energy dissipation phenomenon occurring around embedded graphene nanoplatelets.

In addition, Guo et al.[86] have reported on GNPs-cement mortar with the notable increase of the compressive strength of 65.8%. However, the composition of this particular composite differs significantly from the composites fabricated within other studies, since it involves the use of silane-treated nanoplatelets as well as silica fume and steel slag, therefore the results cannot be directly compared. Indeed, also in this case, as for graphene oxide, the composition of the composites as well as the experimental protocols differ drastically among various studies. However, here, the most crucial aspect affecting the results of mechanical tests is the lateral size and thickness of GNPs flakes varying from 2 μm[59] to 100 μm[56] and from 2 nm[58] to 37 nm,[53] respectively, without the clear correlation between the size of the flakes and the increase or decrease of the strength.

Undoubtedly, the GNPs filling phenomena leads to the refinement of porosity of cement composites as well as increases the tortuosity of pore system in cement matrix. Du and Pang[53] have revealed that the addition of 5 wt.% of GNPs leads to the notable reduction of the average, median and critical pore diameter as well as the fraction of macropores by 10.5%, 27.5%, 33.5% and 10.5%, respectively (Figure 7c). As a result, the successful

application of GNPs in highly durable cement composite was achieved in this study. The GNPs remarkably reinforced the barrier properties of cement mortar, in particular the water penetration depth was reduced from 18.1 mm to 4.4 mm, while the apparent chloride diffusion coefficient was lowered by 40% (Figure 7d).

3.4. FLG/MLG

The research on the cementitious composites incorporating few-layer or multi-layer graphene remains highly limited and involves mainly the evaluation of the electrical properties and sensing ability. However, the pioneering work revealing a great potential of application of graphene in high strength cement composites was published by Silva et al.[66] The cement mortar with 0.033 wt.% loading of MLG with lateral size of 4 μm and thickness in the range of 0.7-20 nm exhibited the unprecedented increase of the tensile strength by 100%, 144% and 132% for specimens cured for 3, 7 and 28 days, respectively, while the MLG addition of 0.021 wt.% improved the compressive strength by 64%, 94% and 96%, respectively. Nevertheless, it should be pointed out that the fabrication protocol of this composite is extremely complex and time-consuming, since the strategy involves (1) pouring the MLG dispersion in isopropanol into dry sand, and (2) the sand storage for 48 h to allow the full evaporation of isopropanol, prior to adding cement and water.

Unlike GO that possesses the oxygen functional groups being the nucleation sites for cement hydration products, graphene provides the accelerated cement hydration due to the sp^2 bonded carbon planes acting as nanonucleation points extensively reacting with hydration crystals (**Figure 8**a).[66,81] In fact, FLG and MLG have emerged as a suitable choice for cement composites, because they combine several beneficial reinforcing mechanisms, such as (1) the refined porosity of cement matrix due to filling phenomena[87,88] (**Figure 9**b, c and d), (2) the accelerated hydration and nucleation of cement hydration products resulting in more compact and uniform microstructure,[66,81,87,88] (3) the bridging effect inhibiting the formation

and propagation of cracks[61,87] (Figure 9e and f) and (4) strong interface bonding strength between hydration products and graphene flakes caused by the friction forces[61,87] (Figure 9a). Moreover, according to Zhao et al.,[87] FLG affects positively the autogenous and drying shrinkage of cement composites most probably due to entrapping of water molecules within graphene layers: the drying shrinkage strain after 30 days was clearly reduced by 27.4%, from -1.79‰ to -1.30‰ for 0.06 wt.% loading of FLG (Figure 8b).

4. Self-sensing ability of graphene-based cementitious composites

Structural Health Monitoring is defined as a process involving continuous, real-time measurements of the state of building structures for ensuring the early diagnosis of damage with the characterization of a damage type and localization as well as for providing an appropriate warning system.[12] Up to date, SHM has been implemented into concrete structures by using various types of sensors attached to the surface of the structure, embedded into it during construction or installed on the reinforcement. However, such sensors suffer from unfavorable compatibility with deforming concrete and thus insufficient durability, high cost, extensive wiring connections, expensive peripheral equipment or, in case of embedded sensors, the degradation of the structural performance of concrete.[12,89] This encourages the scientists worldwide to develop novel cementitious composites with self-sensing capabilities, which become both the structural materials and the durable and inexpensive sensors.[90] The strategy to produce self-sensing concrete relies on the incorporation of a conductive filler, which may form the conductive network within cement matrix enabled to monitor strain, stress, formation of cracks or even construction failure. Therefore, unlike GO, which is electrically insulting, graphene, owing to its outstanding electrical properties,[16] offers a multitude of potential solutions towards the development of self-monitoring cement composites. Up to date, the self-sensing cement materials have been fabricated mostly with

the use of GNPs and FLG, while the effect of rGO on electrical and piezoresistive properties of cementitious composites has not been evaluated yet.

Typically, concrete is considered as an insulting material with the electrical resistivity in the range of 10^3-10^4 kΩ*cm.[55,86,91] Moreover, this value strongly relies on the moisture of cement matrix and water evaporation, since the ionic conduction is dominant in plain cement composites. Therefore, in order to overcome these limitations, it is crucial to determine the percolation threshold of a conductive filler, i.e. the minimum loading of a filler, which stabilizes the continuous conductive path within the composite and provides the tunneling and contact conduction prevailing over the other types of conduction.[92]

In 2014, a seminal work on smart graphene-cement mortar was published by Le et al.[55] The percolation threshold was achieved in this study for 2.4-3.6 vol.% loading of GNPs (10-15 wt.% loading, **Figure 10**a). Such dosage of GNPs resulted in the unprecedented reduction of the electrical resistivity of cement mortar from 10^4 kΩ*cm to 1 kΩ*cm. Noteworthy, the lateral size and thickness of graphene nanoplatelets amounted to 2.6 μm and 2.6 nm, respectively, while their electrical conductivity was determined as 2-3*10^{-3} S/cm. Interestingly, the authors have also extended the scope of their study to the investigation of the fractional change in resistivity for specimens with different notch depths that allowed to formulate the analytical model to predict the crack depth based on the resistivity measurements. Moreover, it is clear that the electrical response to the damage increases together with the increasing notch depth (Figure 10b).

Another seminal work in this field was reported by Sun et al.[91] Here, the percolation threshold was obtained for 2 vol.% loading of graphene flakes with the lateral size of max. 2 μm and the thickness of 1-5 nm. With such graphene loading, the electrical resistivity of cement paste was reduced from 2400 kΩ*cm to ca. 500 kΩ*cm. However, the secondary percolation phenomenon occurred for 8 vol.% loading of graphene nanosheets, eventually achieving a value of the electrical resistivity as low as 20 kΩ*cm for 10 vol.% loading of

FLG. Moreover, the high conductivity of produced cement composites allowed to meticulously monitor their electrical response to the applied compressive loads. Interestingly, the most sensitive piezoresistive response was found for 5 vol.% loading of FLG (Figure 10c), with higher FLG content leading to the slightly deteriorated piezoresistive properties (Figure 10d). This phenomenon was associated with the formation of aggregates and clusters of graphene flakes, when the content of FLG exceeded 5 vol.%.

Interestingly, Liu et al.[85] have revealed the similar results of percolation threshold, i.e., 2.0 vol.%, for the conductive cement mortars incorporating GNPs with the thickness of 5-10 nm and the lateral size of 2-5 μm. Nevertheless, the obtained results are quite surprising due to the relatively low conductivity of GNPs, i.e., 110 S/cm, indicating that most probably the variations of graphene conductivity in the range of 100-3000 S/cm do not affect significantly the resistivity of GNPs-based composites.

In a similar investigation, Tao et al.[57] have presented the piezoresistive investigation on the cement mortar incorporating GNPs with the lateral size of 5-10 μm and the thickness of 3-10 nm. Interestingly, the authors have indicated that the percolation threshold was achieved for the extremely low content of graphene of 0.236 vol.% (GNPs conductivity of 500-1000 S/cm). However, it should be highlighted that the plot presenting the relation between the conductivity and GNPs loading is not displayed in logarithmic scale and this may cause the misinterpretation of the percolation threshold value (Figure 10e). Indeed, this is further confirmed by the piezoresistivity tests, since the response of the material to the applied load was not sufficiently stable and clear for the GNPs loadings investigated within this work.

An additional paramount aspect to consider whenever self-sensing concrete is applied in health monitoring of structures concerns the polarization phenomenon, the fingerprint of the movement and aggregation of ions in cement pore solution. Noteworthy, it was proved that the polarization effect may be also extensively reduced with the application of graphene-based materials: Guo et al.[86] have revealed that with the introduction of 0.05 wt.% of FLG

the polarization time was decreased from 25 s to 15 s (Figure 10f). Moreover, Bai et al. have shown[63] that the incorporation of silica fume to the graphene-based cement composites may significantly increase their conductivity. Indeed, the 2 wt.% loading of FLG resulted in the decrease of the resistivity from 10^3 kΩ*cm to 10 kΩ*cm, while the addition of 15 wt.% of silica fume caused the further reduction of the resistivity by 3 orders of magnitude due to the improved dispersion of graphene within cement matrix.

It is worth mentioning that, in addition to SHM, the sensing ability of graphene-based cementitious composites opens perspective towards some novel, intriguing applications, such as (1) real-time monitoring of the development of chloride-induced corrosion based on the relationship between the chloride ion content and conductivity of graphene-based cement composites, which is separated from the ion conductivity and pH value[93] (**Figure 11**a); (2) building energy harvesting due to the combination of remarkable electrical and thermal properties, in particular the significant improvement of thermoelectric efficiency of cement composites has been achieved[94] (Figure 11b); (3) new electric-induced curing method for cementitious composites envisaged for construction in deep-freeze temperatures.[85]

Intuitively, the high performance, strength and durability as well as the new smart functionalities and the possibility of the application of graphene-cement composites in SHM make them being considered as the environmentally-friendly and sustainable alternative for ordinary concrete.[20,22] Nevertheless, the studies involving the toxicity as well as the environment and health effects of graphene-based cement composites remain highly limited. The pioneering work presenting the environmental effect of using GNPs in cement composites, by means of the attributional Life Cycle Assessment, was published by Papanikolaou et al.[95] The authors have revealed that the production of 1 kg of GNPs by liquid phase exfoliation results in 0.17 $kg_{CO2\ eq}$, while the production of Portland cement leads to the release of 0.86 $kg_{CO2\ eq}$. Additionally, the impact of Portland cement was indicated as 248 times more damaging in terms of global warming and 124 times more harmful for human

health in terms of respiratory inorganics, if compared with the application of GNPs as nanofillers in cementitious composites. Although these results make graphene-family materials promising candidates for the application as concrete nano-additives, further comprehensive research in that field is needed.

5. Summary and outlook

Considering the extraordinary properties of graphene-related materials and enormous progress made in the field over the past decade, we are at the point of entering a new era of materials science that could have high impacts on the systems we develop. These ultrathin materials can be prepared by means of a wide range of well-established methods. In-depth explorations in the field of graphene-related materials also brings new challenges. Their successful introduction into composites mainly depends on the ability to provide any chosen material in large quantities at a reasonable cost. Undoubtedly, graphene-based materials represent a veritable breakthrough in such an exciting area of concrete structures. Yet, the development of an efficient method for obtaining the appropriate and homogenous dispersion of graphene and derivatives thereof within cement matrix is highly desired as well as precise control over size and thickness of graphene sheets remains challenging. Furthermore, the optimization of the graphene production in specific solvents (non-hazardous and eco-friendly) will be the subject of future efforts to allow compatibly with both concrete technologies and safety regulations. Since the first report on cement mortar incorporating graphene oxide appeared in 2013, increasing efforts have been devoted to the enhancement of the performance of GO-based cement composites. Indeed, the composites incorporating the PCE-assisted aqueous dispersion of GO feature with accelerated cement hydration, uniform microstructure and improved mechanical properties, yet the reinforcing mechanism of GO has not been clearly determined. Another pressing problem with GO-cement composites is the extremely high cost of nanomaterials, if compared with the cost of plain concrete, making their industrial

applications unreasonable. Therefore, other graphene derivatives, namely GNPs, rGO, MLG and FLG, should gain considerable attention in developing concrete nanotechnology due to their remarkable electrical conductivity offering the possibility to construct the smart and elegant cement-based structural materials. In fact, from economic point of view, graphene and derivatives thereof may play in the future the leading role in self-sensing cement composites, surpassing even carbon nanotubes, which have been extensively studied in this field so far. In particular, GNPs and FLG have been tested as promising 2D materials for high performance, self-sensing cement composites, however, the beneficial effect of GNPs on microstructure and mechanical properties of cement materials is highly restricted due to their large size. Reduced graphene oxide has been also discussed in this Review as an alternative to GO, however the research involving rGO-cement composites are still in their infancy, showing quite discouraging results. Nevertheless, the investigation of the electrical properties of rGO-cement composites is an additional intriguing research path to discover.

In the future, the development of the efficient, low-cost and technologically simple dispersion method for graphene-based materials still remains the greatest challenge to be tackled in this field. Moreover, the effect of the dispersion method as well as surfactants used needs to be thoroughly investigated. Ultimately, the potential technological applications of graphene-based cement composites require performing large-scale mechanical tests and electrical measurements allowing to establish the designing and monitoring protocols. Of significant importance is also to unambiguously determine the influence of the graphene sheets size and thickness on the electrical properties and piezoresistive response of cementitious composites. Moreover, it appears to be particularly important to investigate also the long-term effect of graphene-based materials on mechanical and durability-related properties of cementitious composites. Further research on toxicity and environmental impact of graphene-based cement composites is crucial from the human health and safety perspective. Finally, the integration of graphene and related materials to concrete technology

can also allow to impart new functions to the composites in order to create smart buildings holding unprecedented features. Noteworthy, the concepts presented in this Review can be also extended to the use of other 2D materials, which possess a broadest portfolio of physical properties and therefore offer the possibility to further tune next-generation smart structures.

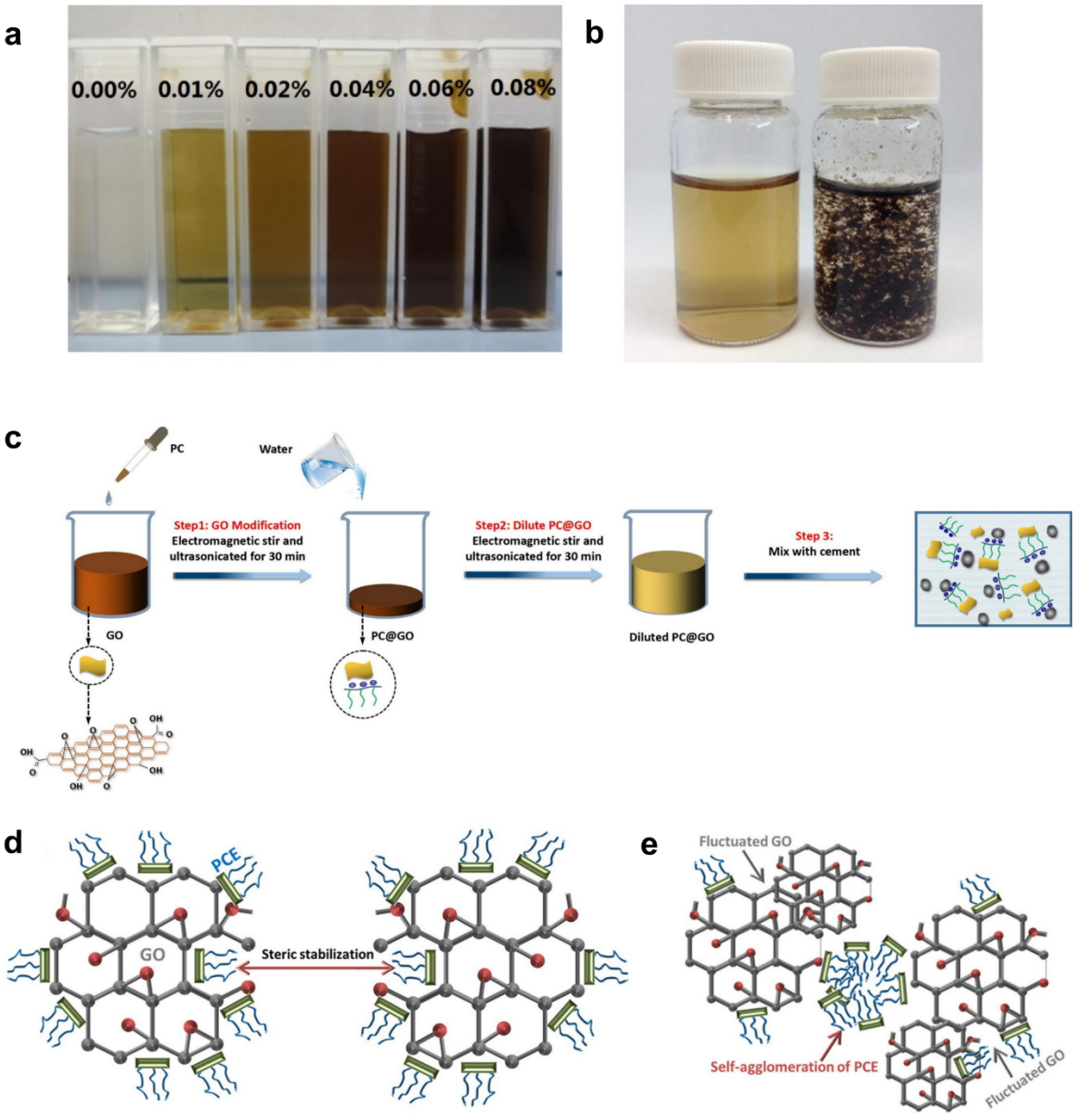

Figure 1. Commonly adopted protocols for obtaining uniform GO dispersion within cement matrix. a) Aqueous dispersion with various loadings of GO after sonication. Reproduced with permission.[30] 2017, Elsevier. b) GO dispersion before (left) and after (right) the addition of $Ca(OH)_2$ solution. Reproduced with permission.[38] 2016, Elsevier. c) Fabrication protocol for cement composites incorporating GO functionalized by PCE. Reproduced with permission.[74] 2018, Elsevier. d) Steric stabilization and e) self-aggregation of GO-PCE dispersion. Reproduced with permission.[42] 2017, Elsevier.

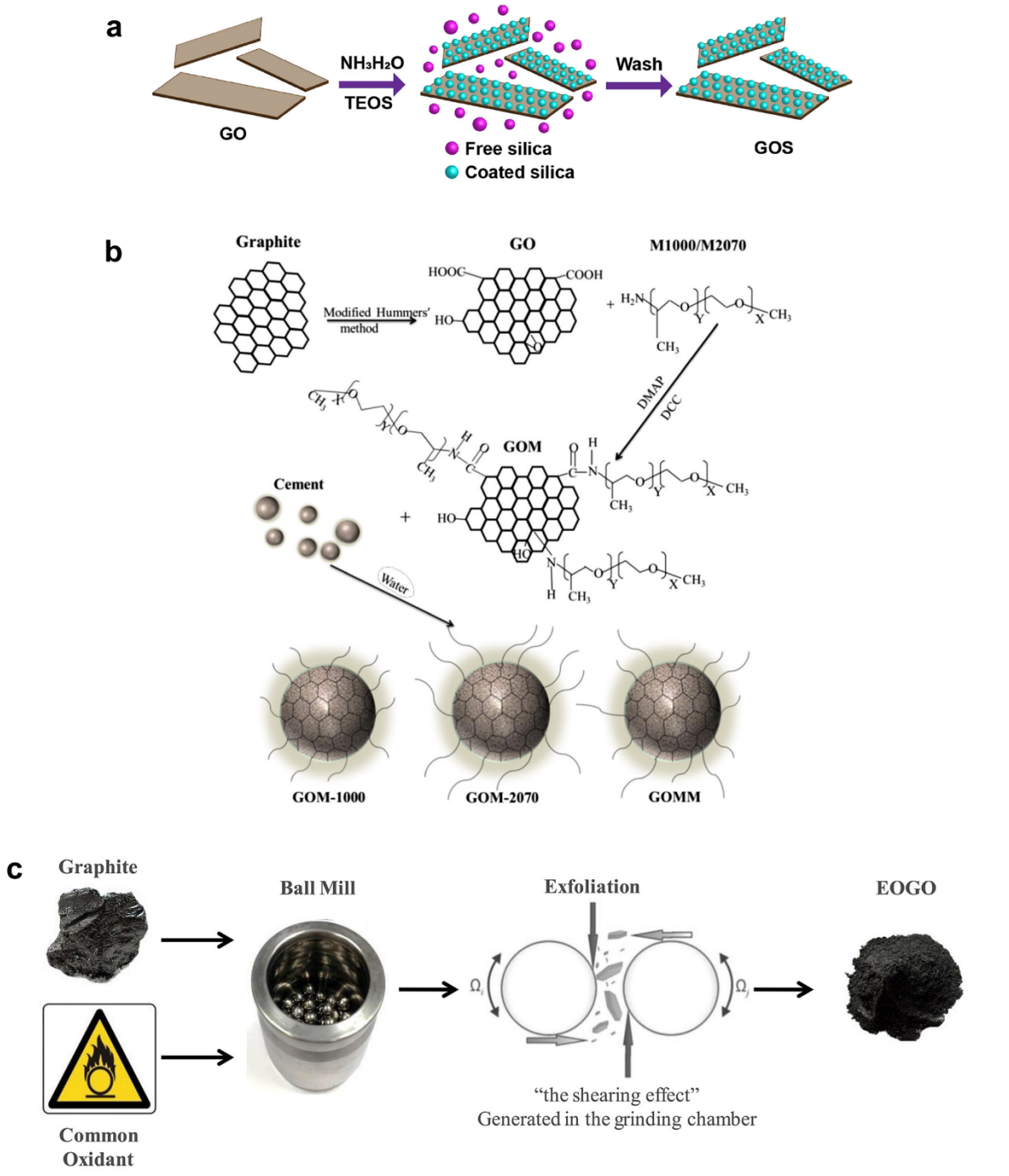

Figure 2. Additional strategies for dispersing GO within cement matrix: a) Synthesis of GOS nanohybrids. Reproduced with permission.[47] 2020, Elsevier. b) Chemical functionalization of GO by polyether amines. Reproduced with permission.[49] 2017, Elsevier. c) Production of the edge-oxidized graphene oxide by ball-milling treatment. Reproduced with permission.[51] 2019, Elsevier.

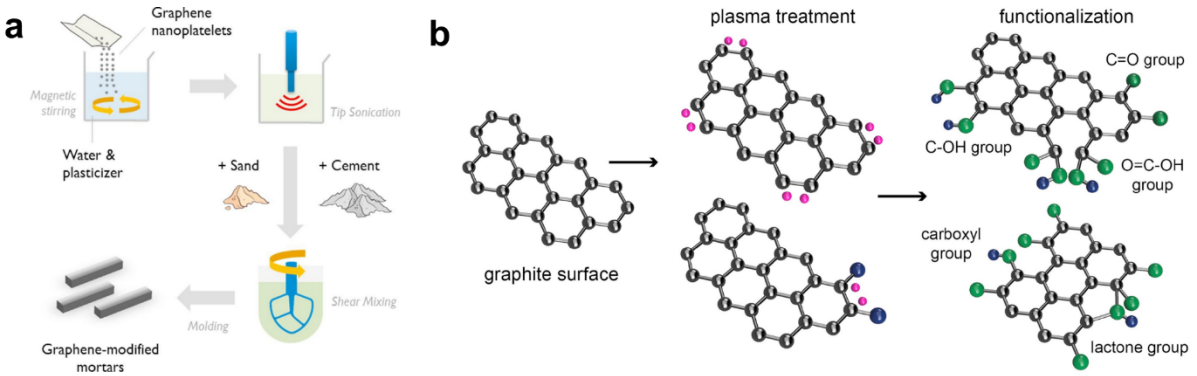

Figure 3. Fabrication strategies for graphene-based cementitious composites: a) Manufacturing process involving the use of superplasticizers. Reproduced with permission.[58] 2019, Elsevier. b) O_2 plasma functionalization of graphite. Reproduced with permission.[67] 2019, Elsevier.

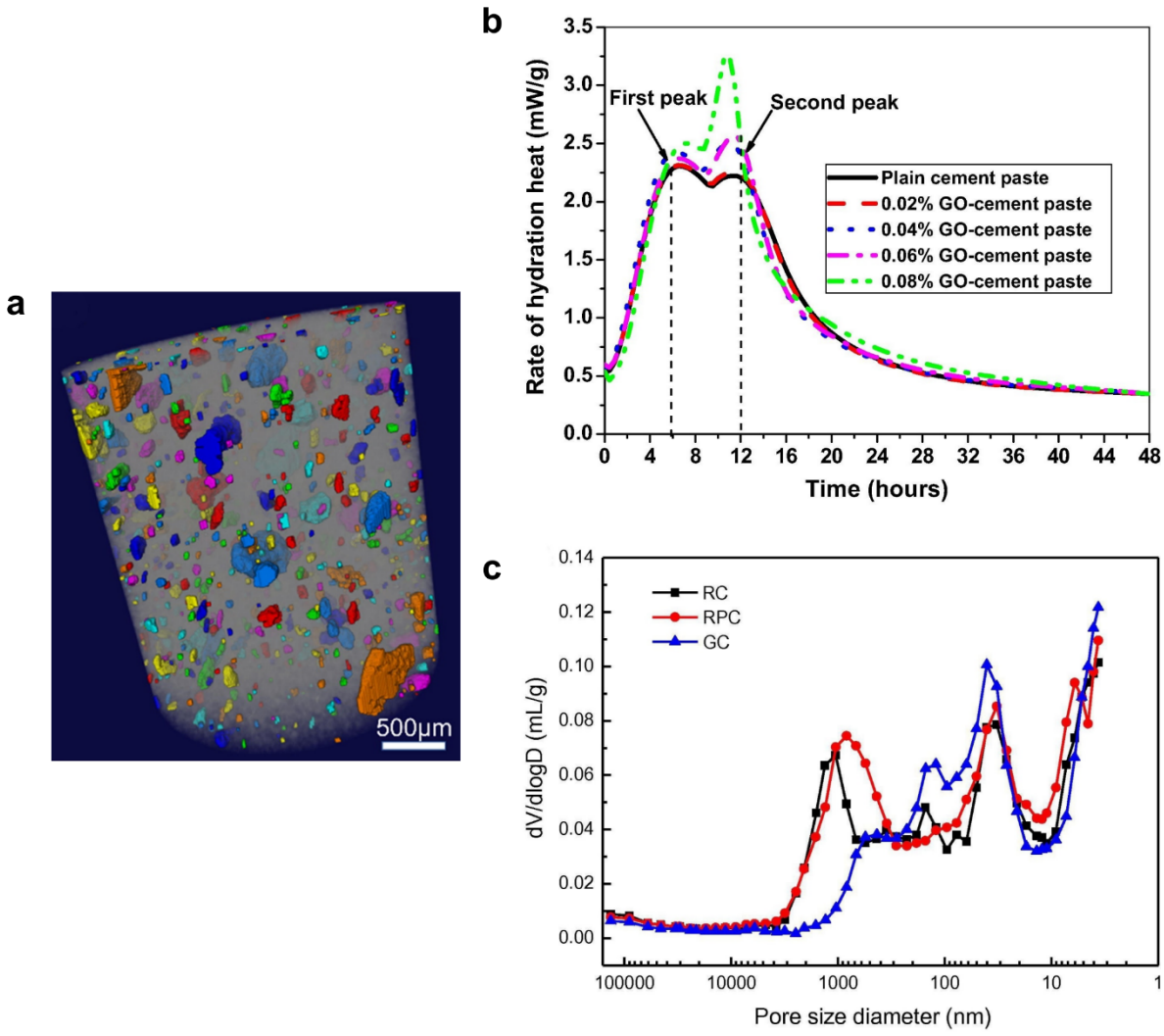

Figure 4. Microstructural characterization of GO-cement composites. a) Spatial distribution model of GO agglomerations in cement matrix. Reproduced with permission.[72] 2020, Elsevier. b) Rate of heat released during hydration of GO-cement composites. Reproduced with permission.[30] 2017, Elsevier. c) Differential pore size distribution curves for RC – cement paste, RPC – cement paste with PC, GC – GO-cement paste with PC. Reproduced with permission.[74] 2018, Elsevier.

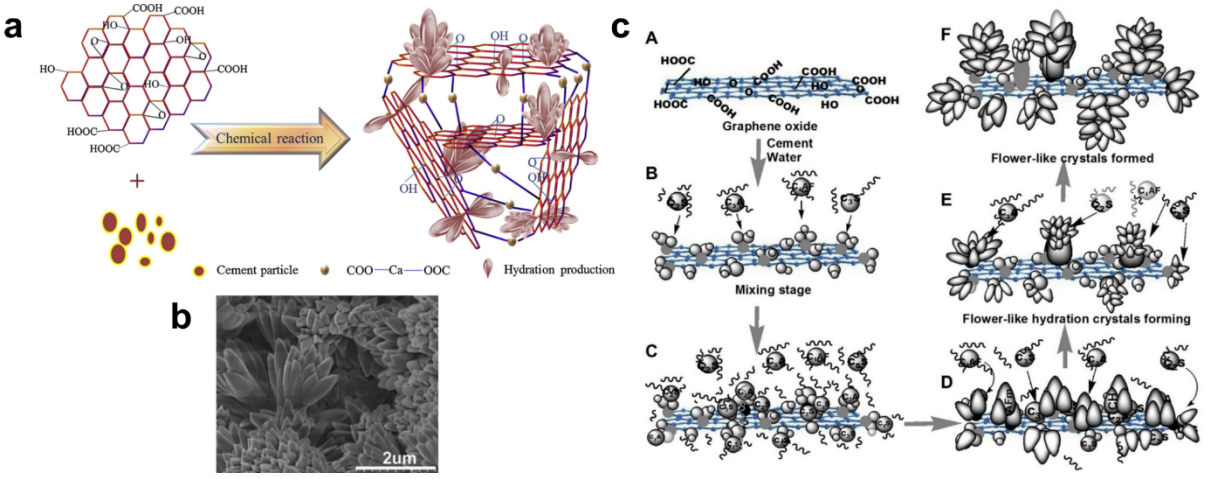

Figure 5. Reinforcing mechanisms proposed for GO-cement composites. a) 3D model of GO-based cement composite with a new hydration product $Ca(HCOO)_2$. Reproduced with permission.[28] 2016, Elsevier. b) Flower-like hydration crystals and c) their formation on GO nanosheets. Reproduced with permission.[24] 2013, Elsevier.

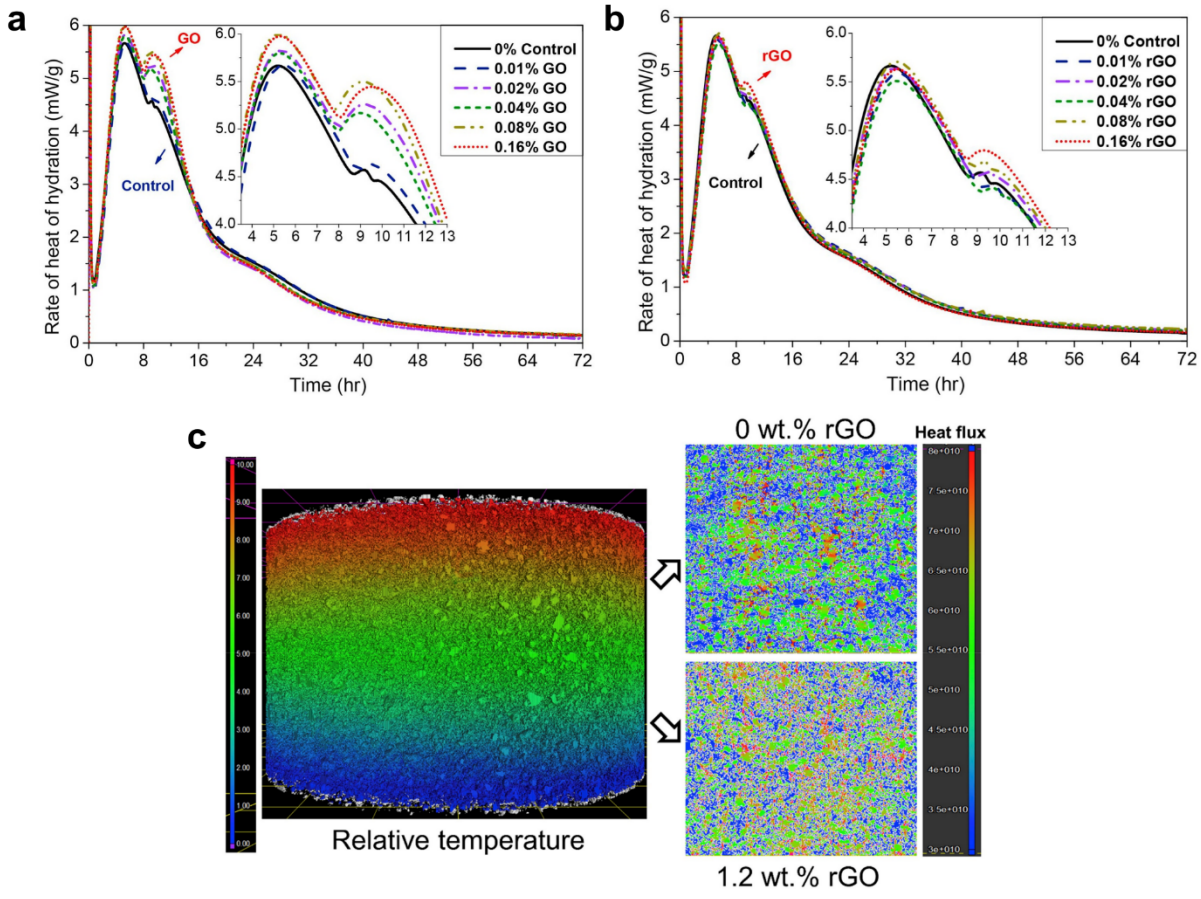

Figure 6. Microstructural characterization of rGO-cement composites. a) and b) Rate of hydration heat for cement composites incorporating a) GO and b) rGO. Reproduced with permission.[81] 2020, Elsevier. c) Relative temperature field (left) and heat flux fields (right) for plain cement mortar and mortar with rGO. Reproduced with permission.[84] 2020, Elsevier.

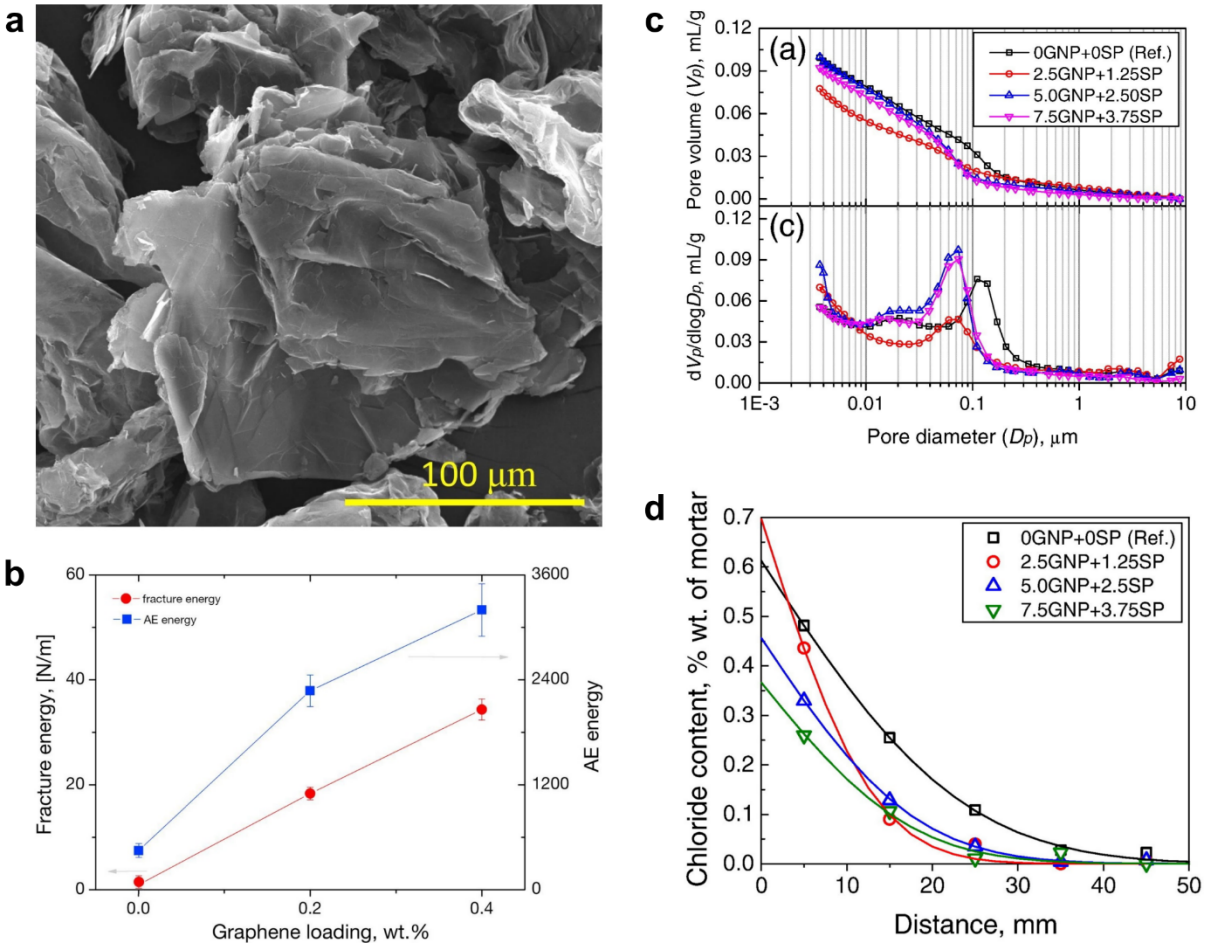

Figure 7. Mechanical and microstructural characterization of GNPs-cement composites. a) SEM image of GNP. Reproduced with permission.[56] 2020, Elsevier. b) Acoustic emission and fracture energy during flexural tests of GNPs-cement composites. Reproduced with permission.[58] 2019, Elsevier. c) Cumulative pore volume curves and d) spatial distribution of chloride content in cement mortars incorporating GNPs. Reproduced with permission.[53] 2015, Elsevier.

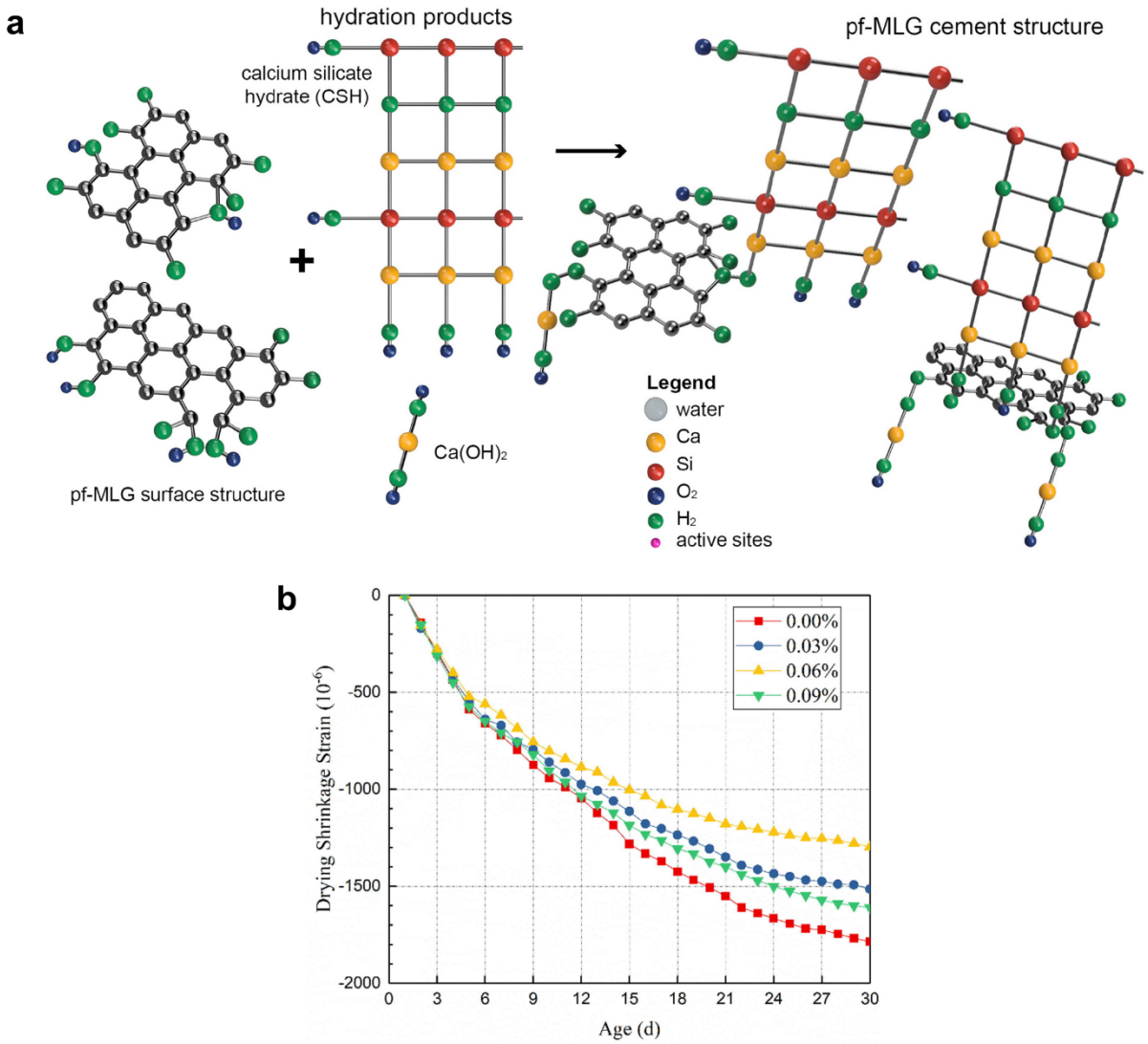

Figure 8. Microstructural and mechanical characterization of cement composites incorporating FLG and MLG. a) Effect of O_2 plasma functionalized MLG on cement hydration. Reproduced with permission.[67] 2019, Elsevier. b) Drying shrinkage of FLG-cement composites. Reproduced with permission.[87] 2020, Elsevier.

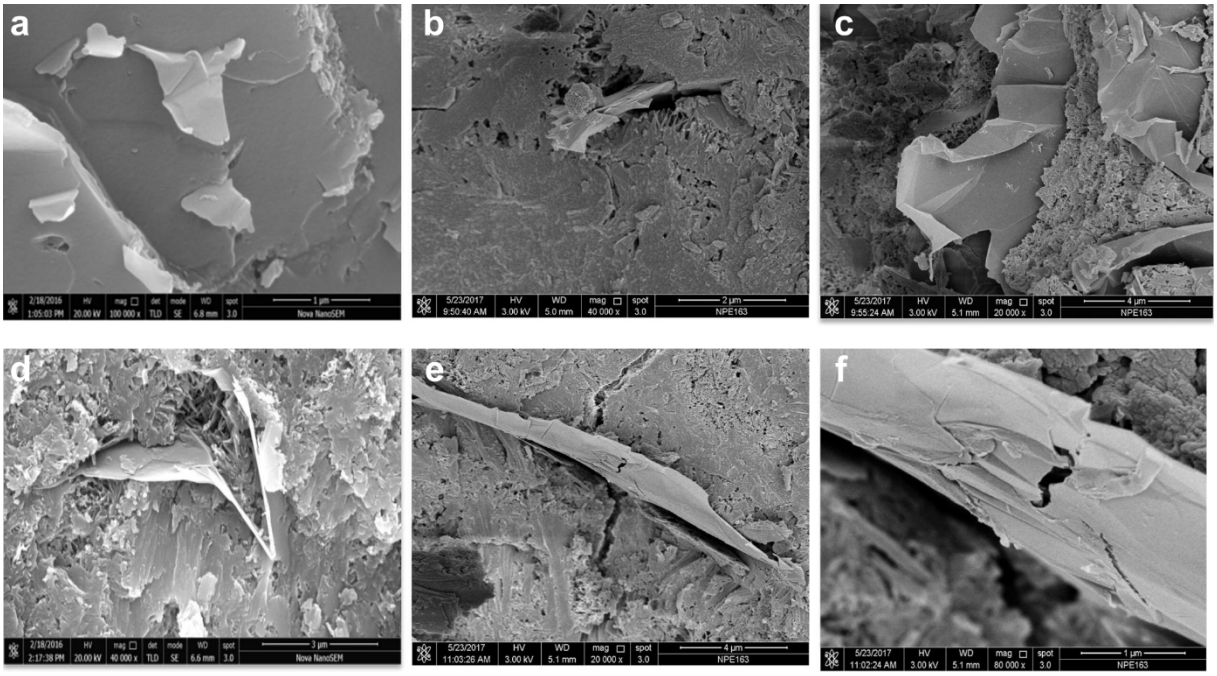

Figure 9. SEM images of cement composites incorporating MLG: a) MLG flakes visible on the fracture surface of cement matrix, b), c) and d) graphene filling and barrier phenomena, e) and f) MLG crack-arresting phenomenon. Reproduced with permission.[88] 2018, Elsevier.

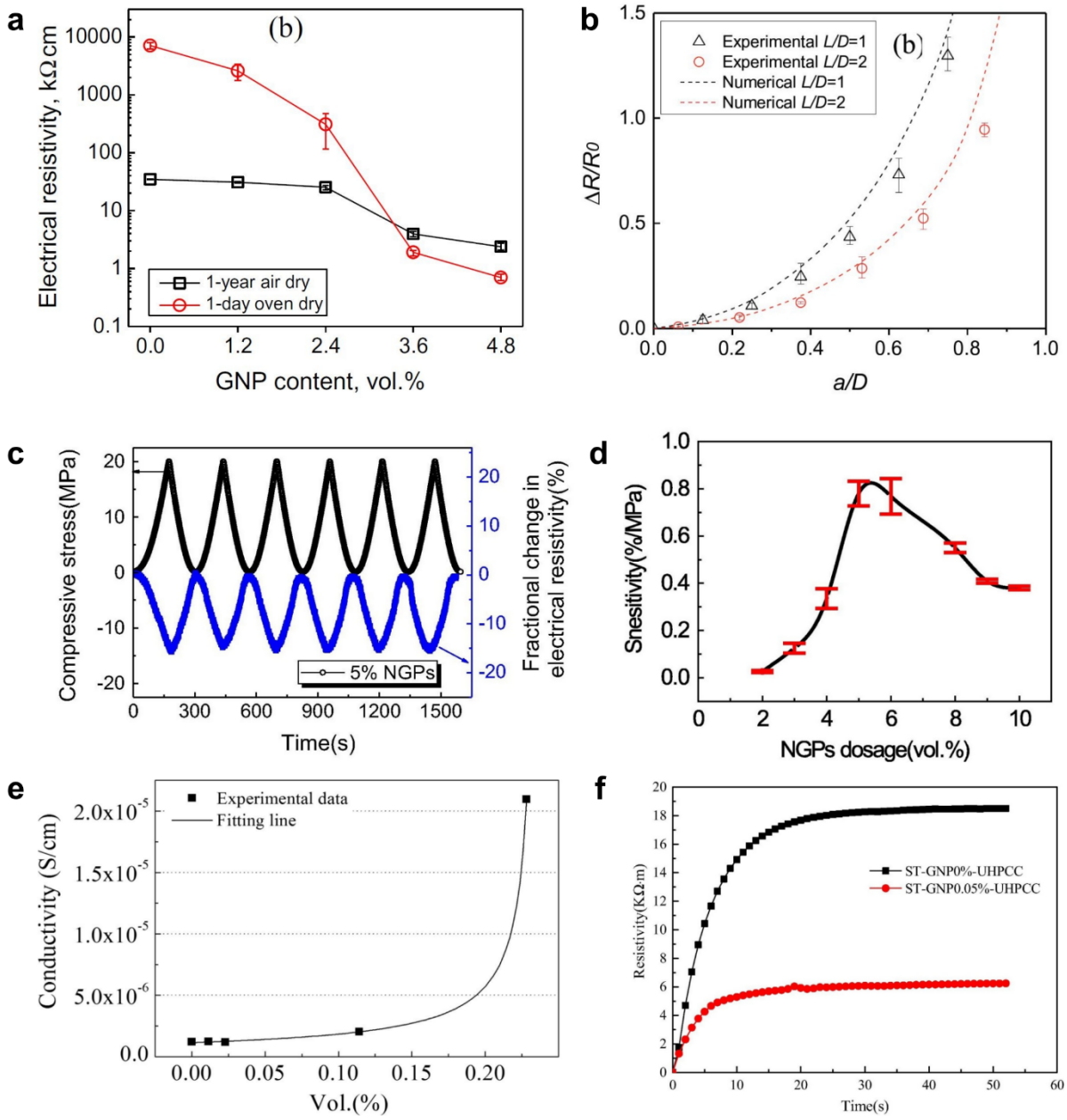

Figure 10. Electrical and piezoresistivity measurements of graphene-based cement composites. a) Electrical resistivity in relation to GNPs loading and b) resistivity changes in specimens with different notch depth for GNPs-cement mortars. Reproduced with permission.[55] 2014, Elsevier. c) and d) Fractional changes of resistivity in FLG-cement pastes. Reproduced with permission.[91] 2017, Elsevier. e) Electrical resistivity in GNPs-modified cement mortars. Reproduced with permission.[57] 2019, Elsevier. f) Polarization effect in ultra-high strength concrete reinforced with GNPs. Reproduced with permission.[86] 2020, Elsevier.

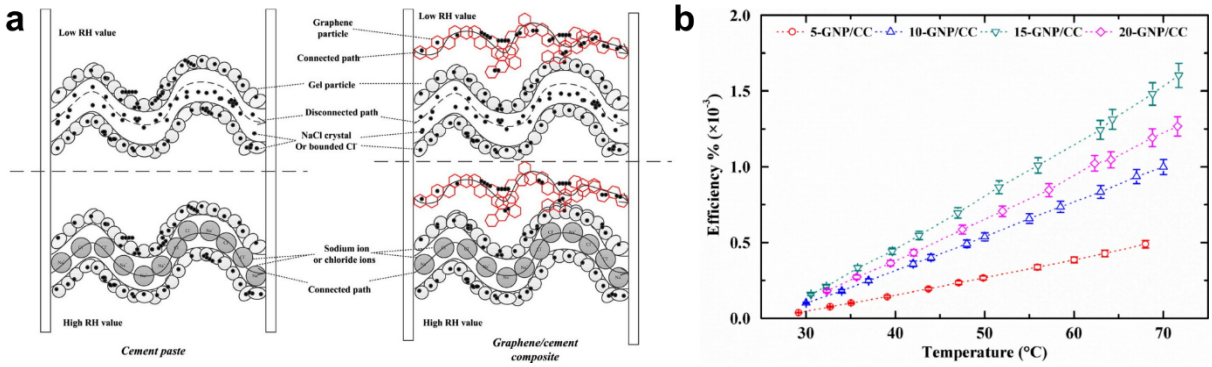

Figure 11. a) Conductive paths in cement paste and graphene-based cement composite during chloride-induced corrosion. Reproduced with permission.[93] 2017, Elsevier. b) Thermoelectric efficiency of graphene-cement composite for fixed cold side temperature at 25 °C. Reproduced with permission.[94] 2019, Elsevier.

Acknowledgements
We acknowledge financial support from the Polish National Science Center (Grant No. 2019/33/NST5/00832), the European Commission through the Graphene Flagship Core 3 project (GA-881603), as well as the Agence Nationale de la Recherche through the Labex project CSC (ANR-10-LABX-0026 CSC) within the Investissement d'Avenir program (ANR-10-120 IDEX-0002-02), the International Center for Frontier Research in Chemistry (icFRC) and the University of Strasbourg Institute for Advanced Study (USIAS).

Conflict of Interest
The authors declare no conflict of interest.

Received: ((will be filled in by the editorial staff))
Revised: ((will be filled in by the editorial staff))
Published online: ((will be filled in by the editorial staff))

References

[1] G. Habert, S. A. Miller, V. M. John, J. L. Provis, A. Favier, A. Horvath, K. L. Scrivener, *Nat. Rev. Earth Environ.* **2020**, *1*, 559.

[2] P. J. M. Monteiro, S. A. Miller, A. Horvath, *Nat. Mater.* **2017**, *16*, 698.

[3] H. Manzano, A. N. Enyashin, J. S. Dolado, A. Ayuela, J. Frenzel, G. Seifert, *Adv. Mater.* **2012**, *24*, 3239.

[4] EN 1992-1-1: 2004 Eurocode 2: Design of concrete structures - Part 1-1: General rules and rules for Buildings, **2008**, 29.

[5] D. W. Hobbs, *Int. Mater. Rev.* **2001**, *46*, 117.

[6] S. A. Miller, A. Horvath, P. J. M. Monteiro, *Nat. Sustain.* **2018**, *1*, 69.

[7] A. M. Neville, *Properties of concrete. 5th Edition.*, Pearson Education Limited, Harlow, England, **2011**.

[8] Z. Li, *Advanced Concrete Technology*, Wiley, Hoboken, NJ, USA, **2011**.

[9] D. D. L. Chung, *Mater. Today* **2002**, *5*, 30.

[10] S. Chuah, Z. Pan, J. G. Sanjayan, C. M. Wang, W. H. Duan, *Constr. Build. Mater.* **2014**, *73*, 113.

[11] J. Lee, S. Mahendra, P. J. J. Alvarez, *ACS Nano* **2010**, *4*, 3580.

[12] M. J. Hanus, A. T. Harris, *Prog. Mater. Sci.* **2013**, *58*, 1056.

[13] V. Palermo, *Chem. Commun.* **2013**, *49*, 2848.

[14] A. K. Geim, K. S. Novoselov, *Nat. Mater.* **2007**, *6*, 183.

[15] F. Bonaccorso, A. Lombardo, T. Hasan, Z. Sun, L. Colombo, A. C. Ferrari, *Mater. Today* **2012**, *15*, 564.

[16] V. Singh, D. Joung, L. Zhai, S. Das, S. I. Khondaker, S. Seal, *Prog. Mater. Sci.* **2011**, *56*, 1178.

[17] J. Kim, L. J. Cote, J. Huang, *Acc. Chem. Res.* **2012**, *45*, 1356.

[18] H. Yang, H. Cui, W. Tang, Z. Li, N. Han, F. Xing, *Compos. Part A Appl. Sci. Manuf.* **2017**, *102*, 273.

[19] Y. Xu, J. Zeng, W. Chen, R. Jin, B. Li, Z. Pan, *Constr. Build. Mater.* **2018**, *171*, 291.

[20] E. Shamsaei, F. Basquiroto, D. Souza, X. Yao, E. Benhelal, A. Akbari, W. Duan, *Constr. Build. Mater.* **2018**, *183*, 642.

[21] K. Chintalapudi, R. M. R. Pannem, *Constr. Build. Mater.* **2020**, *259*, 120598.

[22] L. Zhao, X. Guo, L. Song, Y. Song, G. Dai, J. Liu, *Constr. Build. Mater.* **2020**, *241*, 117939.

[23] A. Anwar, B. S. Mohammed, M. bin Abdul Wahab, M. S. Liew, *Dev. Built Environ.*

2019, *1*, 100002.

[24] S. Lv, Y. Ma, C. Qiu, T. Sun, J. Liu, Q. Zhou, *Constr. Build. Mater.* **2013**, *49*, 121.

[25] M. M. Mokhtar, S. A. Abo-El-Enein, M. Y. Hassaan, M. S. Morsy, M. H. Khalil, *Constr. Build. Mater.* **2017**, *138*, 333.

[26] E. Horszczaruk, E. Mijowska, R. J. Kalenczuk, M. Aleksandrzak, S. Mijowska, *Constr. Build. Mater.* **2015**, *78*, 234.

[27] A. Mohammed, J. G. Sanjayan, W. H. Duan, A. Nazari, *Constr. Build. Mater.* **2015**, *84*, 341.

[28] M. Wang, R. Wang, H. Yao, S. Farhan, S. Zheng, C. Du, *Constr. Build. Mater.* **2016**, *126*, 730.

[29] X. Li, Y. M. Liu, W. G. Li, C. Y. Li, J. G. Sanjayan, W. H. Duan, Z. Li, *Constr. Build. Mater.* **2017**, *145*, 402.

[30] W. Li, X. Li, S. J. Chen, Y. M. Liu, W. H. Duan, S. P. Shah, *Constr. Build. Mater.* **2017**, *136*, 506.

[31] Z. Lu, X. Li, A. Hanif, B. Chen, P. Parthasarathy, J. Yu, Z. Li, *Constr. Build. Mater.* **2017**, *152*, 232.

[32] D. Hou, Z. Lu, X. Li, H. Ma, Z. Li, *Carbon* **2017**, *115*, 188.

[33] X. Li, Z. Lu, S. Chuah, W. Li, Y. Liu, W. H. Duan, Z. Li, *Compos. Part A Appl. Sci. Manuf.* **2017**, *100*, 1.

[34] Q. Wang, X. Cui, J. Wang, S. Li, C. Lv, Y. Dong, *Constr. Build. Mater.* **2017**, *138*, 35.

[35] Z. Pan, L. He, L. Qiu, A. H. Korayem, G. Li, J. W. Zhu, F. Collins, D. Li, W. H. Duan, M. C. Wang, *Cem. Concr. Compos.* **2015**, *58*, 140.

[36] T. S. Qureshi, D. K. Panesar, *Constr. Build. Mater.* **2019**, *206*, 71.

[37] S. Chuah, W. Li, S. J. Chen, J. G. Sanjayan, W. H. Duan, *Constr. Build. Mater.* **2018**, *161*, 519.

[38] X. Li, A. H. Korayem, C. Li, Y. Liu, H. He, J. G. Sanjayan, W. H. Duan, *Constr. Build.*

Mater. **2016**, *123*, 327.

[39] H. Yang, M. Monasterio, H. Cui, N. Han, *Compos. Part A Appl. Sci. Manuf.* **2017**, *102*, 263.

[40] L. Zhao, S. Zhu, H. Wu, X. Zhang, Q. Tao, L. Song, Y. Song, X. Guo, *Constr. Build. Mater.* **2020**, *247*, 118446.

[41] L. Zhao, X. Guo, C. Ge, Q. Li, L. Guo, X. Shu, J. Liu, *Compos. Part B Eng.* **2017**, *113*, 308.

[42] Z. Lu, A. Hanif, C. Ning, H. Shao, R. Yin, Z. Li, *Mater. Des.* **2017**, *127*, 154.

[43] W.-J. Long, T. Ye, Y.-C. Gu, H.-D. Li, F. Xing, *Constr. Build. Mater.* **2019**, *202*, 177.

[44] X. Yan, D. Zheng, H. Yang, H. Cui, M. Monasterio, Y. Lo, *Constr. Build. Mater.* **2020**, *257*, 119477.

[45] Y. Shang, D. Zhang, C. Yang, Y. Liu, Y. Liu, *Constr. Build. Mater.* **2015**, *96*, 20.

[46] M. Hu, J. Guo, P. Li, D. Chen, Y. Xu, Y. Feng, Y. Yu, H. Zhang, *Constr. Build. Mater.* **2019**, *225*, 745.

[47] J. Lin, E. Shamsaei, F. Basquiroto de Souza, K. Sagoe-Crentsil, W. H. Duan, *Cem. Concr. Compos.* **2020**, *106*, 103488.

[48] R. Mowlaei, J. Lin, F. Basquiroto de Souza, A. Fouladi, A. Habibnejad Korayem, E. Shamsaei, W. Duan, *Constr. Build. Mater.* **2021**, *266*, 121016.

[49] M. Wang, H. Yao, R. Wang, S. Zheng, *Constr. Build. Mater.* **2017**, *150*, 150.

[50] G. Jing, J. Wu, T. Lei, S. Wang, V. Strokova, V. Nelyubova, M. Wang, Z. Ye, *Constr. Build. Mater.* **2020**, *248*, 118699.

[51] J. An, B. H. Nam, Y. Alharbi, B. H. Cho, M. Khawaji, *Compos. Part B Eng.* **2019**, *173*, 106795.

[52] H. Du, S. D. Pang, *Constr. Build. Mater.* **2018**, *167*, 403.

[53] H. Du, S. D. Pang, *Cem. Concr. Res.* **2015**, *76*, 10.

[54] B. Wang, B. Pang, *Constr. Build. Mater.* **2019**, *226*, 699.

[55] J.-L. Le, H. Du, S. D. Pang, *Compos. Part B Eng.* **2014**, *67*, 555.

[56] J. Wang, J. Tao, L. Li, C. Zhou, Q. Zeng, *Compos. Part A Appl. Sci. Manuf.* **2020**, *130*, 105750.

[57] J. Tao, X. Wang, Z. Wang, Q. Zeng, *Constr. Build. Mater.* **2019**, *209*, 665.

[58] I. Tragazikis, K. G. Dassios, P. T. Dalla, D. A. Exarchos, T. E. Matikas, *Eng. Fract. Mech.* **2019**, *210*, 444.

[59] J. Liu, J. Fu, Y. Yang, C. Gu, *Constr. Build. Mater.* **2019**, *199*, 1.

[60] M. Muthu, M. Santhanam, *Cem. Concr. Compos.* **2018**, *91*, 118.

[61] V. D. Ho, C. T. Ng, C. J. Coghlan, A. Goodwin, C. Mc Guckin, T. Ozbakkaloglu, D. Losic, *Constr. Build. Mater.* **2020**, *234*, 117403.

[62] W. Baomin, D. Shuang, *Constr. Build. Mater.* **2019**, *228*, 116720.

[63] S. Bai, L. Jiang, N. Xu, M. Jin, S. Jiang, *Constr. Build. Mater.* **2018**, *164*, 433.

[64] B. Wang, R. Jiang, Z. Wu, *Nanomaterials* **2016**, *6*, 200.

[65] J. Xu, D. Zhang, *Cem. Concr. Compos.* **2017**, *84*, 74.

[66] R. A. Silva, P. Castro Guetti, M. S. Luz, F. Rouxinol, R. V. Gelamo, *Constr. Build. Mater.* **2017**, *149*, 378.

[67] M. S. D. C. Dela Vega, M. R. Vasquez, *Compos. Part B Eng.* **2019**, *160*, 573.

[68] M. Krystek, D. Pakulski, V. Patroniak, M. Górski, L. Szojda, A. Ciesielski, P. Samorì, *Adv. Sci.* **2019**, *6*, 1801195.

[69] M. Krystek, *PhD Thesis*, Silesian University of Technology, July, **2019**.

[70] X. Li, L. Wang, Y. Liu, W. Li, B. Dong, W. H. Duan, *Cem. Concr. Compos.* **2018**, *92*, 145.

[71] K. Chintalapudi, R. M. R. Pannem, *J. Build. Eng.* **2020**, *32*, 101551.

[72] G. Jing, K. Xu, H. Feng, J. Wu, S. Wang, Q. Li, X. Cheng, Z. Ye, *Constr. Build. Mater.* **2020**, *264*, 120729.

[73] M. Birenboim, R. Nadiv, A. Alatawna, M. Buzaglo, G. Schahar, J. Lee, G. Kim, A.

Peled, O. Regev, *Compos. Part B Eng.* **2019**, *161*, 68.

[74] L. Zhao, X. Guo, Y. Liu, Y. Zhao, Z. Chen, Y. Zhang, L. Guo, X. Shu, J. Liu, *Constr. Build. Mater.* **2018**, *190*, 150.

[75] K. Vallurupalli, W. Meng, J. Liu, K. H. Khayat, *Constr. Build. Mater.* **2020**, *265*, 13.

[76] H. Peng, Y. Ge, C. S. Cai, Y. Zhang, Z. Liu, *Constr. Build. Mater.* **2019**, *194*, 102.

[77] L. Zhao, D. Hou, P. Wang, X. Guo, Y. Zhang, J. Liu, J. Zhang, *Constr. Build. Mater.* **2020**, *257*, 119566.

[78] W.-J. Long, Y. Gu, B.-X. Xiao, Q. Zhang, F. Xing, *Constr. Build. Mater.* **2018**, *179*, 661.

[79] A. Mohammed, J. G. Sanjayan, A. Nazari, N. T. K. Al-Saadi, *Constr. Build. Mater.* **2018**, *168*, 858.

[80] W.-J. Long, Y. Gu, F. Xing, K. H. Khayat, *Cem. Concr. Compos.* **2018**, *94*, 72.

[81] T. S. Qureshi, D. K. Panesar, *Compos. Part B* **2020**, *197*, 108063.

[82] A. Gholampour, M. Valizadeh Kiamahalleh, D. N. H. Tran, T. Ozbakkaloglu, D. Losic, *ACS Appl. Mater. Interfaces* **2017**, *9*, 43275.

[83] S. Prabavathy, K. Jeyasubramanian, S. Prasanth, G. S. Hikku, R. B. J. Robert, *J. Build. Eng.* **2020**, *28*, 101082.

[84] G. Jing, Z. Ye, J. Wu, S. Wang, X. Cheng, V. Strokova, V. Nelyubova, *Cem. Concr. Compos.* **2020**, *109*, 103559.

[85] Y. Liu, M. Wang, W. Wang, *Mater. Des.* **2018**, *160*, 783.

[86] L. Guo, J. Wu, H. Wang, *Constr. Build. Mater.* **2020**, *240*, 117926.

[87] Y. Zhao, Y. Liu, T. Shi, Y. Gu, B. Zheng, K. Zhang, J. Xu, Y. Fu, S. Shi, *Constr. Build. Mater.* **2020**, *257*, 119498.

[88] B. Wang, R. Zhao, *Constr. Build. Mater.* **2018**, *161*, 715.

[89] B. Han, X. Yu, J. Ou, B. Han, X. Yu, J. Ou, In *Self-Sensing Concrete in Smart Structures*, Elsevier, **2014**, pp. 189–230.

[90] Z.-Q. Shi, D. D. . Chung, *Cem. Concr. Res.* **1999**, *29*, 435.

[91] S. Sun, B. Han, S. Jiang, X. Yu, Y. Wang, H. Li, J. Ou, *Constr. Build. Mater.* **2017**, *136*, 314.

[92] B. Han, X. Yu, J. Ou, B. Han, X. Yu, J. Ou, In *Self-Sensing Concrete in Smart Structures*, Elsevier, **2014**, pp. 163–187.

[93] M. Jin, L. Jiang, M. Lu, S. Bai, *Constr. Build. Mater.* **2017**, *136*, 394.

[94] S. Ghosh, S. Harish, K. A. Rocky, M. Ohtaki, B. B. Saha, *Energy Build.* **2019**, *202*, 109419.

[95] I. Papanikolaou, N. Arena, A. Al-Tabbaa, *J. Clean. Prod.* **2019**, *240*, 118202.